Automated Finishing of Organ Models Created by 3D Printing

Yoshihide Tamaki[1], Kohji Niwa[2], Anthony Beaucamp[3] and Yoshimi Takeuchi[4]
[1,4]Dept. of Mechanical Engineering, Graduate School of Engineering, Chubu University, Japan
[2]DMG MORI Co. Ltd., Japan [3]Dept. of Micro-Engineering, Kyoto University, Japan
[1]tm17009-1268@sti.chubu.ac.jp, [4]takeuchi_yoshimi@isc.chubu.ac.jp

Abstract:
In recent years, transparent resin organ models created by 3D printing have found application in the medical field. The inside of the organ model contains diseased parts, blood vessels and so on, but they cannot be seen due to the layered appearance of printed surfaces. To address this issue, an automated system was developed using an industrial robot to replace the manual polishing currently needed. The automated system consists of three aspects: fixturing of the organ model, polishing tool path generation, and polishing process conditions. From polishing experiments on a relatively simple shape, it was found that the system has the potential to deliver transparent surfaces on complex resin organ models.

Keywords: Polishing, Organ model, Resin, Robot, Tool path generation

1. Introduction

In recent years, the topic of 3D printing (also known as additive manufacturing) has been frequently in the limelight. Although 3D printers themselves are not a new technology, they have become widespread owing to lower prices and easier operation. Thus, transparent resin organ models created by 3D printing are used for investigation, operation, etc. in the medical field. While currently used in only a few medical institutions, there is a strong case for they use in delivering higher quality medical care, and so demand is expected to increase in the future.

Since the organ model, containing diseased parts, blood vessels, etc. is created layer by layer on the 3D printer, it is impossible to see the inside due to the fine step-like surface roughness. For this reason, a polishing operation with sponges containing abrasives is required to smooth the organ model, followed by pasting of a varnish such that the inside of the organ model can be seen. Although research on 3D printing has been actively pursued [1], little work on post-processing has been done so far, after generation of the 3D printed objects. Furthermore, while polishing of metallic artifacts has often been considered [2][3], there are few examples of resin polishing.

Consequently, this research deals with the development of an automated finishing system using industrial robots instead of the current manual polishing operation which is very time consuming. In the present study, the most popular liver resin model was selected among several organ models. The liver has numerous irregularities on its surface, making it an extremely challenging free-form shape. Such liver resin model is shown in Fig. 1, before and after finishing by hand.

The proposed automated system consists of three aspects: (1) fixturing of the organ model, (2) polishing path generation by CAM system, and (3) polishing process conditions.

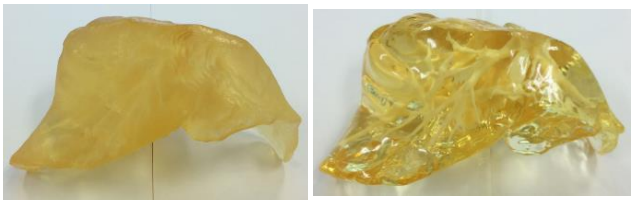

(a) Before polishing (b) After manual polishing

Figure 1: Human liver model created by 3D printing

2. System configuration

The outline of the proposed system is shown in Fig. 2. Human organ models are created by 3D printing on the basis of STL files generated from X-ray CT scan data. Our proprietary CAM system, named ChubuCAM, generates the polishing path from the STL data of human organ models. The polishing path data is transferred from the PC to the robot controller (RC8) using ORiN2, the connection interface, then the robot initiates polishing operations.

The equipment used in the experiment is a vertical articulated robot (VS-060) manufactured by DENSO WAVE INC. The robot has an arm reach of 605 mm and load capacity of 4 kg, making it compact and with 6 degrees of freedom. This allows tool posturing in a wide range of position/orientation.

The polishing unit (an air driven spindle with maximum rotation speed 7000 rpm and torque of 0.22 Nm, an air cylinder, and rotating tool) is attached to the robot plate.

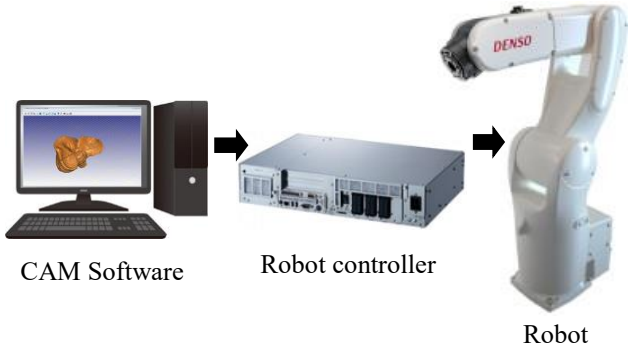

Figure 2: System configuration

3. Fixturing of organ model

It is very difficult for the robot to polish every facets of the liver model due to constraints on the movable range of the robot. Thus, a rotating fixture device supporting the liver model from two sides is required. However, as can be seen from Fig. 1, the surface of the liver model has a complex curvature. Although a method using low melting temperature metals or the like has been reported as a fixturing method in cutting complicated shapes [4][5], it is not applicable here because the glass transition temperature of the resin is 77 to 80° C.

For this reason, a fixture and rotating device were designed to hold the liver model. Two holders have the reverse shapes of the liver model in the grasped area, and are created by 3D printing. These holders with reverse shape are obtained by Boolean operation between the liver data and the cylindrical data on a part of the holder.

Figure 3 shows STL data of two holders generated by using our CAM system. Figure 4 shows the actual holders created by a 3D printer (Stratasys FORTUS 360mc-L). The material used was ABS-M30, and the laminating pitch was 0.127 mm. Figure 5 shows actual fixturing of the liver model. The current device can be manually rotated every 60 degrees, however automatic rotation is planned in future.

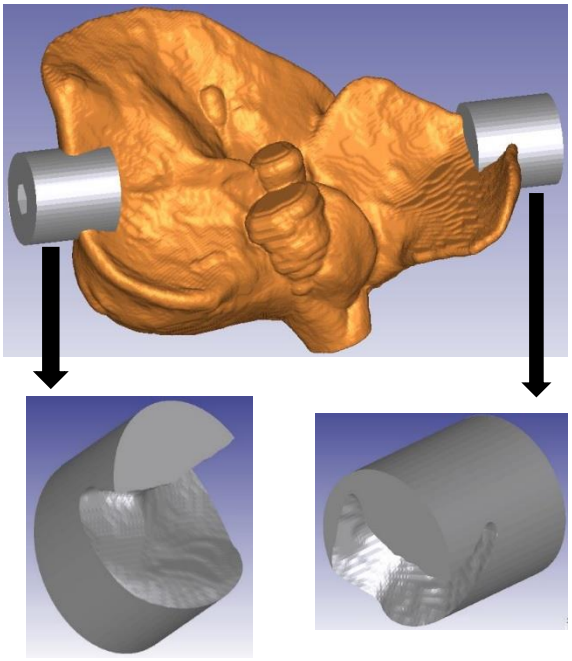

Figure 3: Holders with reverse shape of liver model

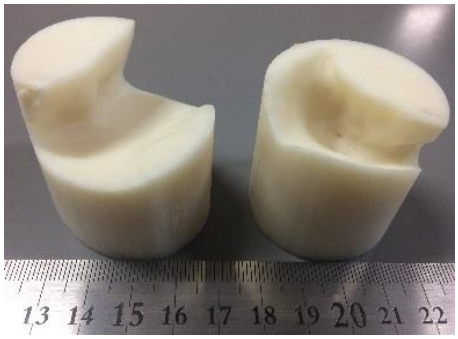

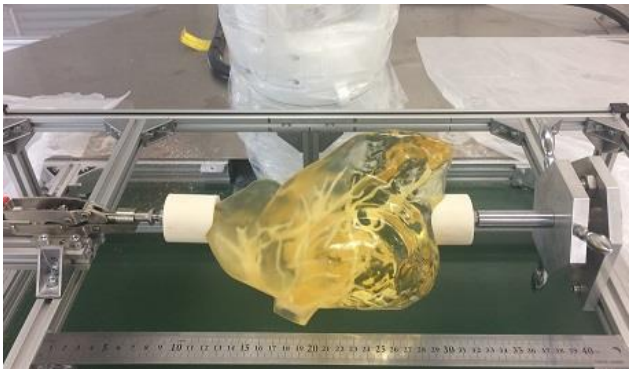

Figure 4: Actual 3D printed holders

Figure 5: Appearance of complete fixturing device

4. Polishing path generation

4.1 Division of polishing area

Unlike STEP and IGES, the operator cannot easily select specific surfaces in STL meshes (Standard Triangulated Language). Therefore, according to the fixturing method, the liver model is divided into six areas every 60 degrees, with the aim of polishing the whole model in sub-sections. The division is done as follows;

1. Fig. 6 (a) shows a 60-degree fan-shaped columnar body covering the organ model. Using the same Boolean method explained in Fig. 3, the intersecting volume is extracted as shown in Fig. 6(b).
2. In Fig. 6(b), the liver model faces are necessary, however the sides of the fan-shaped columnar are not necessary, thus deleting a large number of small triangles on both sides. As both sides are plane, the coordinates of the center of gravity for each triangle in the STL data are calculated. If they are located in the plane, these triangles are eliminated. Finally, the organ surface is isolated, as illustrated in Fig. 6(c).

Six areas are automatically created by repeating this process 6 times. During the step shown in Fig. 6(c), small isolated areas can appear after deletion of the 60-degree columnar. This may occur when the back side of the model intrudes into the columnar during intersection. These back side parts are gathered together and deleted as shown in Fig. 6(d). The whole shape is finally sub-divided, as shown in Fig. 6(e).

4.2 Polishing path generation with constant spacing

In the present study, polishing path generation is done based on X-axis scanning curves. X-axis scanning curve generation is carried out with constant pickfeed, however the path spacing of areas inclining more towards the Y-axis direction becomes wider, as shown in Fig. 7. When this scanning line processing is applied to the liver model as it is, insufficient polishing and residual defects may take place. Therefore, it is necessary to generate paths with spacing kept at a constant value.

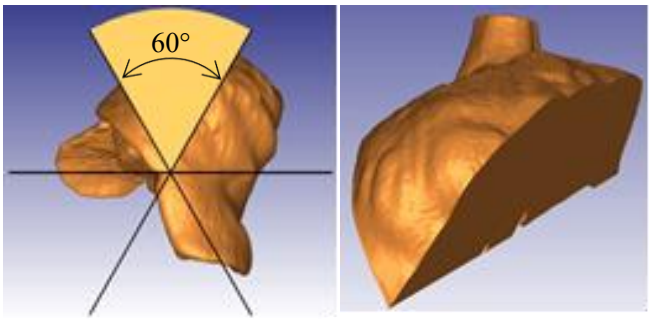

(a) Extraction by Boolean intersection

(b) Extracted result

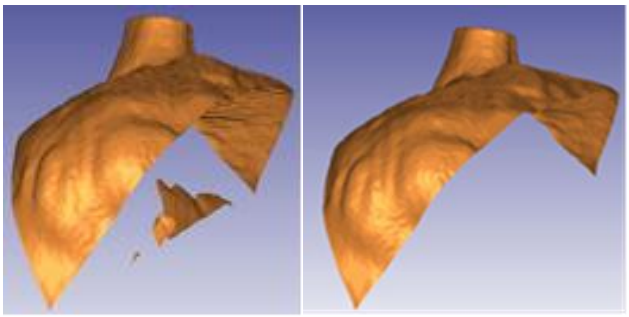

(c) Deletion of columnar faces

(d) Removal of areas belonging to back side

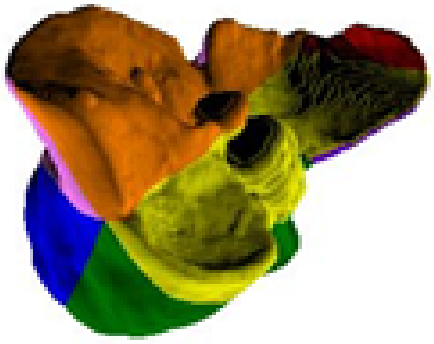

(e) Entire liver model sub-divided into 6 areas

Figure 6: Division process

ChubuCAM generates the polishing points, together with their normal and tangent vectors, along section planes. The amount of pickfeed with regard to the polishing path is determined, as illustrated in Fig. 8. All the normal vectors are projected on the XZ plane, and a vector is created in the XZ plane. Then, the angle θ between the normal vector and the XZ vector is obtained at each point of the path. It can be inferred that the polishing point with the maximum angle has the most inclination to the Y-axis direction and thereby path distance there becomes the widest. Then, an outer product vector is created in the positive Y-axis direction from the normal vector and the tangent vector at the point. The next track is located by multiplying an arbitrary pickfeed by the Y component of the outer product vector.

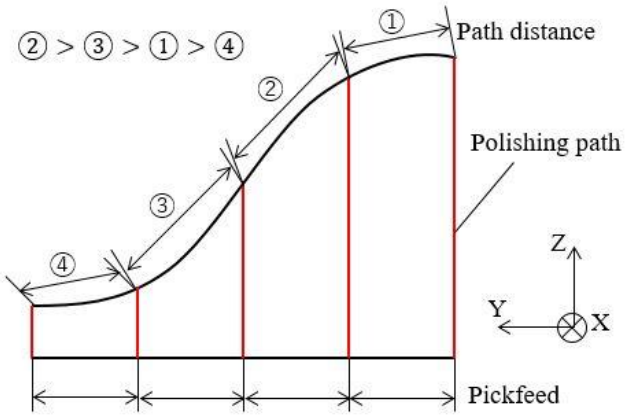

Figure 7: State of pickfeed and path distance

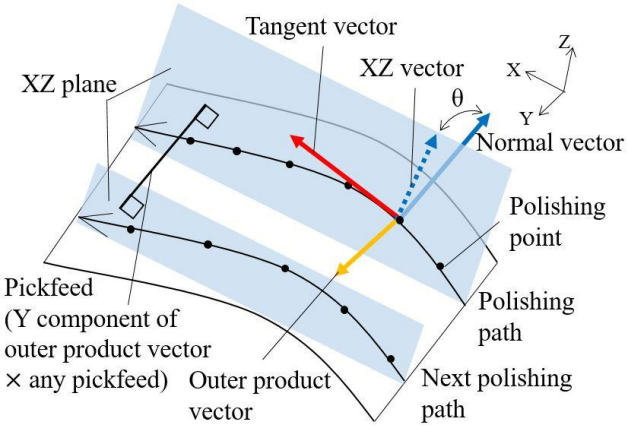

Figure 8: Determination of the next track

In the above method, path distance can be kept constant with respect to the slope of linear segments, however it cannot be kept in areas where the surface curvature changes suddenly. Therefore, successive tracks generated by the above method are calculated on the basis of the distance to the preceding track. The path distance is set to be within ± 10 % of the allowable range. When exceeding this value, a new track is regenerated. As shown in Fig. 9, the pairs of point on track 2 that are closest from given points on track 1, are sought and the distance to the straight line composed of the pair of points is calculated. This is done at all polishing points of track 1, and the maximum value is taken as the path distance.

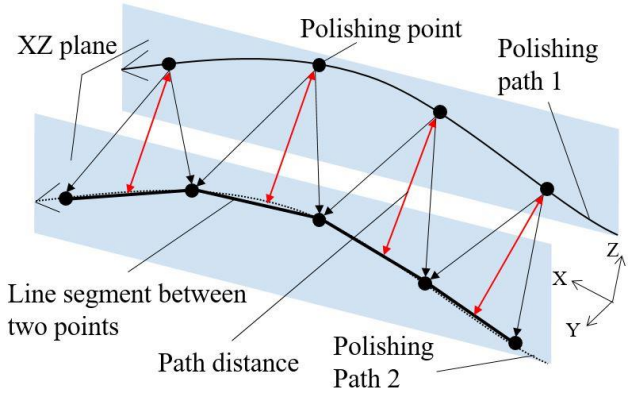

Figure 9: Determination of path distance

As shown in Fig. 10, a polishing point having the maximum path distance and a plane having its tangent vector as the normal vector are created. Then, an intersection line between the plane and the triangular mesh of the object is created in the Y-axis positive direction from the point. Then, the shortest distance along the intersection line from this point is calculated to the nearest point that matches the pickfeed. As a result, a polishing path is generated, where the path distance is kept smaller than the given amount of pickfeed.

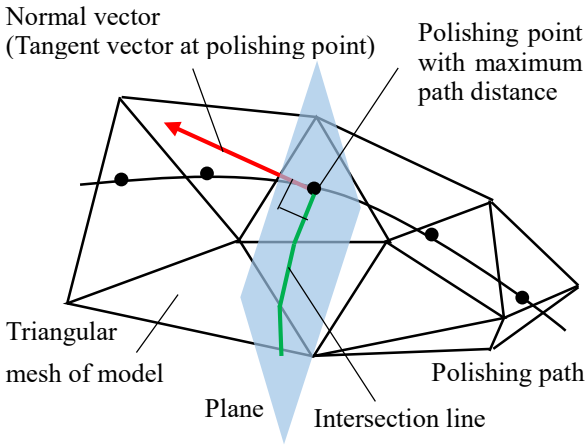

Figure 10: Intersection of plane and triangular mesh

4.3 Comparison of polishing paths

Comparison is made between polishing paths generated by the above method and those generated by conventional methods. Both pickfeeds are set to 2 mm, and a polishing path is generated for the free-form surface as seen in Fig. 11(a). Figures 11(b) and (c) show the results of usual X-axis scanning line processing with constant pickfeed and X-axis scanning line processing with constant track distance, respectively.

From Fig. 11 (c), it is confirmed that an intersection line is created at the point where the path distance becomes widest, as illustrated with the green lines.

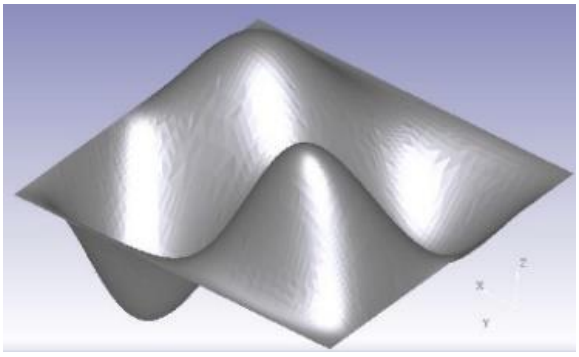

(a) Example of free-form surface

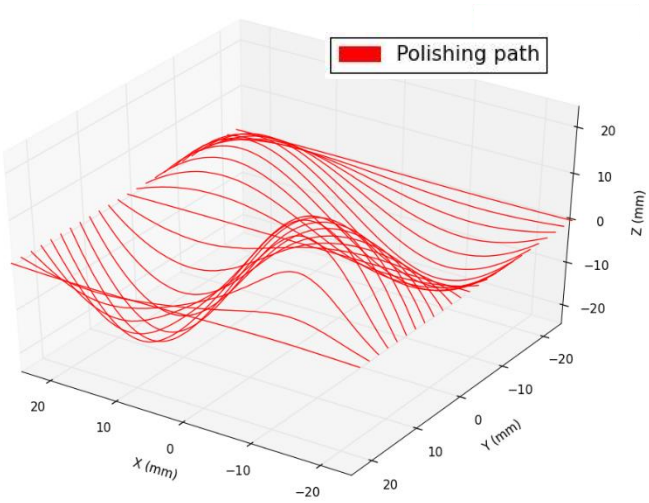

(b) X-axis scanning lines with constant pickfeed

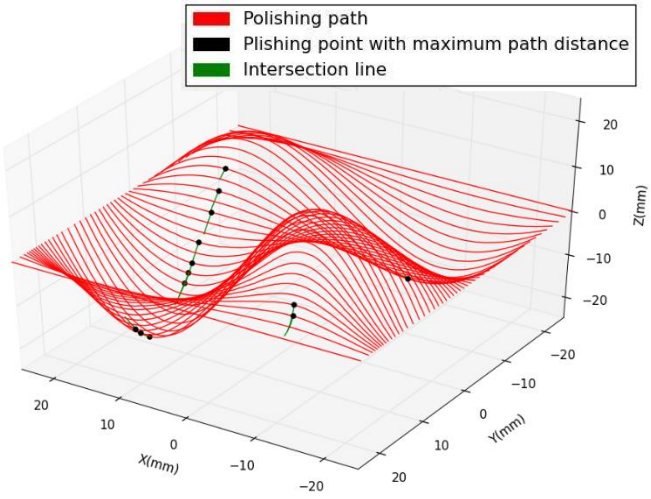

(c) X-axis scanning lines with constant track distance

Figure 11: Comparison of path generation methods

5. Polishing tool selection

The liver model was created on a Agillista 3100 (KEYENCE CO.) 3D printer using AR-M2 transparent resin material. Since polishing of this material has not been reported previously, the selection of an optimal tool was attempted through polishing experiments. Since the liver model is a complicated shape, a tool that adapts to the complicated surface should be employed.

The tools used in the polishing experiments are shown in Fig. 12. In order from left to right, the polishing tools are (a) Daiwarabin #120 (DAIWA KASEI KOGYO Co. Ltd.), (b) rubber wheels #800 (Yanase Co.), (c) Delight wheels #600 (ICHIGUCHI CO.), (d) nylon brush containing abrasives #320 (NAKANISHI INC.) and SAG tools with (e) Nickel Bonded Diamond (NBD) of 9 μm grit, (f) Resin Bonded Diamond (RBD) of 3 μm grit (Zeeko Ltd).

Next, a simple workpiece was created by the same condition as the liver model, for use in the polishing experiment, as shown in Fig. 13. It has a spherical surface of curvature 60 mm. The width is 50 mm.

(a) (b) (c) (d) (e) (f)

Figure 12: Polishing tools

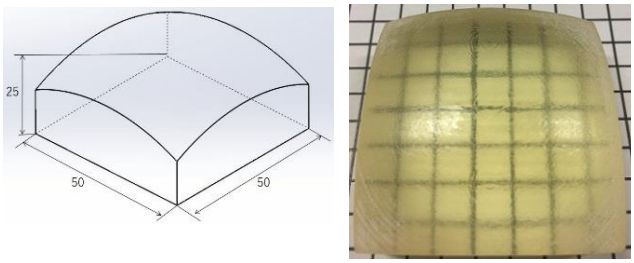

Figure 13: Simple work for polishing experiments

5.1 Polishing Experiments

TPpolishing by use of tools in Fig. 12(a), (b), (c) and (d) was performed at various spindle speeds: 5180 and 6650 rpm, depth of cut: 0.1, 0.2, 0.3 mm, and feed speed: 2.5, 5.1, 7.6 mm/s. The results are summarized as follows:

Fig.12(a): The polished surface showed bad scarring and was obviously rough.

Fig.12(b): The tool got easily worn, lamination pitch and support material cannot be removed.

Fig.12(c): In spite of polishing along the shape, the surface was cut too much since the resin material is too soft.

Fig.12(d): The surface was almost unchanged.

Polishing conditions for the tools shown in Fig. 12(e) and (f) were set with reference to [6], as shown in Table 1. Since SAG is easily affected by heat, feed speed was set to a high value. The polishing process is performed by SAG NBD in both the X-axis and Y-axis feed directions, and repeated twice. Thereafter, SAG RBD processing was performed in the same way.

Figure 14(a) and (b) shows the result of polishing with SAG NBD and SAG RBD, respectively. From Fig. 14(a), it can be confirmed that the lamination pitch and the support material have been removed, although tool marks remained. In Fig. 14(b), the marks were almost completely removed. Surface roughness (Ra) before polishing was 1.67µm, whereas after polishing it was 0.30 µm and a good surface finish could be obtained.

Table 1: polishing condition

Spindle speed	6370 rpm
Depth of cut	0.3 mm
Feed speed	375.6 mm/s
Pick feed	0.3 mm
Angle	20°
Tool path mode	Scanning line processing

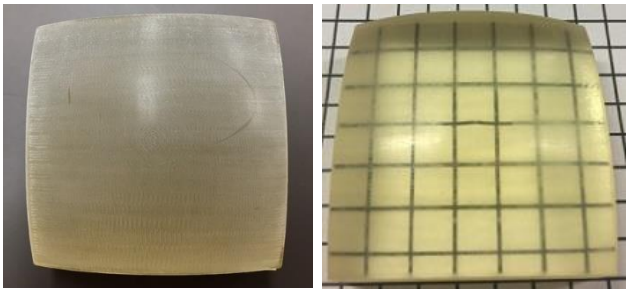

(a) After SAG NBD 9 µm (b) After SAG RBD 3µm

Figure 14: Polishing result with SAG tools

6. Conclusion

This study aimed at developing an automated finishing system for organ models created by 3D printing. The results are summarized as follows:

(1) From polishing path generation with constant track distance, division of polishing area and fixation of the model, it was shown that the system has the potential of producing transparent surfaces on resin organ models.

(2) From the polishing experiments, it was found that SAG tools are the most suitable process for the AR-M2 material.

References

[1] Mori, K., Oda, M., Hayashi, Y., Nimura, Y., Nakata, Y., Kitasaka, T., 2014, Study on organ model fabrication by 3D printer and its application, IEICE technical report, Vol. 113, No. 410, pp. 181-186 (in Japanese)

[2] Morishige, K., Ueki, Y., Ishida, T., Yoshimi, T., 2005, Automation of Polishing Process with Industrial Robots - Polishing Path Generation in Consideration of Surface Curvature -, Proc. of Int. Conf. on Leading Edge Manufacturing in 21st Century (LEM21), Vol.1, pp. 109-114.

[3] Nagata, F., Watanabe K., 2006, Feed Rate Control Using Fuzzy Reasoning for a Mold Polishing Robot, Journal of Robotics and Mechatronics, Vol. 18, No. 1, pp. 76-82.

[4] Obara, H., Watanabe, T., Ohusmi, T., Hatano, M., Ninomiya, E., 2002, A Method to Machine Three-Dimensional Thin Parts, Initiatives of Precision Engineering at the Beginning of a Millennium, pp. 87-91.

[5] Nakamoto, K., Ueji, R., Takeuchi, Y., 2013, Dexterous Machining of Soft Objects Difficult to Clump, Transactions of the Japan society of mechanical engineers, Vol.79, No. 808 (Series C), pp. 4535-4542 (in Japanese).

[6] Beaucamp, A., Namba, Y., Charlton, P., Jain, S., Graziano, A., 2015, Finishing of additively manufactured titanium alloy by shape adaptive grinding (SAG), Surface Topography: Metrology and Properties, 3(2), pp. 024001-8.